ACS ES&T Water

Open Access

pubs.acs.org/estwater

Article

Development of the Channelized Optical System II for *In Situ*, High-Frequency Measurements of Dissolved Inorganic Carbon in Seawater

Mallory Ringham, Zhaohui Aleck Wang,* Frederick Sonnichsen, Steven Lerner, Glenn McDonald, and Jonathan Pfeifer

Cite This: *ACS EST Water* 2024, 4, 1775−1785

Read Online

ACCESS | Metrics & More | Article Recommendations

ABSTRACT: This study describes the development of the CHANnelized Optical System II (CHANOS II), an autonomous, *in situ* sensor capable of measuring seawater dissolved inorganic carbon (DIC) at high frequency (up to ∼1 Hz). In this sensor, CO_2 from acidified seawater is dynamically equilibrated with a pH-sensitive indicator dye encapsulated in gas-permeable Teflon AF 2400 tubing. The pH in the CO_2 equilibrated indicator is measured spectrophotometrically and can be quantitatively correlated to the sample DIC. Ground-truthed field data demonstrate the sensor's capabilities in both time-series measurements and surface mapping in two coastal sites across tidal cycles. CHANOS II achieved an accuracy and precision of ±5.9 and ±5.5 μmol kg^{-1}. The mean difference between traditional bottle and sensor measurements was −3.7 ± 10.0 (1σ) μmol kg^{-1}. The sensor can perform calibration *in situ* using Certified Reference Materials (CRMs) to ensure measurement quality. The coastal time-series measurements highlight high-frequency variability and episodic biogeochemical shifts that are difficult to capture by traditional methods. Surface DIC mapping shows multiple endmembers in an estuary and highlights fine-scale spatial variabilities of DIC. The development of CHANOS II demonstrates a significant technological advance in seawater CO_2 system sensing, which enables high-resolution, subsurface time-series, and profiling deployments.

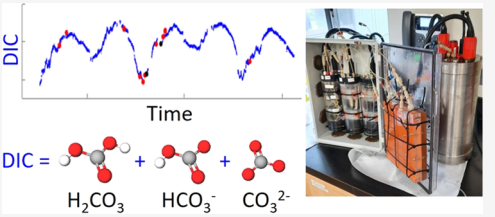

KEYWORDS: *dissolved inorganic carbon, carbon dioxide, sensor, in situ, ocean acidification, carbonate system, carbon cycle*

INTRODUCTION

The study of the marine CO_2 system is critical for understanding global carbon cycling and the impacts of changing ocean chemistry, such as ocean acidification (OA), on marine ecosystems.[1−4] High-resolution, *in situ* measurements of dissolved inorganic carbon (DIC) are valuable for a wide range of seawater carbonate chemistry related studies, including assessing impacts of OA and the fast-growing research in measurement and verification of marine carbon dioxide removal (mCDR) methods.[5−8] DIC may be paired with total alkalinity (TA), pCO_2, or pH to fully constrain the marine CO_2 system with low calculation uncertainty relative to other pairings.[3,9,10] DIC measurements relying on traditional bottle sample analyses are constrained by the speed, workload, and cost of both sample collection and laboratory analysis. However, there are currently no commercially available *in situ* DIC sensors. While DIC analytical methods range from coulometry[11] to membrane introduction mass spectrometry,[12,13] only four *in situ* seawater DIC sensing systems have been published to date, all with reported *in situ* precisions and accuracies approaching climate quality measurements (Table 1).[7,14−18]

In all *in situ* DIC methods, the first common procedure is to acidify seawater to convert all carbonate species to dissolved CO_2, followed by different CO_2 detection methods. In the conductometric method, CO_2 is diffused through a semi-permeable membrane from acidified seawater into a base solution (NaOH), in which reactions between CO_2 and OH^- cause solution conductivity to decrease proportionally to the content of dissolved CO_2, thus DIC in seawater. This method was demonstrated on the first *in situ*, autonomous DIC sensor, the Robotic Analyzer for the TCO_2 System (RATS).[19] This method's small sample requirement (<100 μL) may allow for use on miniaturized sensors, including Lab-on-Chip designs.[20,21]

In the nondispersive infrared absorption (NDIR) method, CO_2 is purged from an acidified sample with a carrier gas (such as N_2- or CO_2-free air) and detected via infrared spectropho-

Received: December 8, 2023
Revised: February 29, 2024
Accepted: February 29, 2024
Published: March 25, 2024

https://doi.org/10.1021/acsestwater.3c00787
ACS EST Water 2024, 4, 1775−1785

Table 1. Summary of Published Prototype *In Situ* DIC Sensing Systems

measurement principle	sensors	*In situ* precision and accuracy (μmol kg^{-1})	measurement cycle time	reported time-series deployment time
conductometry	robotic analyzer for the TCO_2 system (RATS). (RATS)[19]	±2.7 & ±3.6	Hourly	~8 weeks dock deployment
nondispersive infrared absorption (NDIR)	moored autonomous DIC (MADIC) system[15]	±5 & ±6−7	~12 min	~7 month surface mooring deployment
spectrophotometry	spectrophotometric elemental analysis system (SEAS) for DIC (SEAS-DIC)[17]	±2 & ±2	~9 min preparation followed by every ~50 s measurement	~8 day dock deployment
spectrophotometry	CHANnelized Optical System (CHANOS)[18]	±2.5 & ±5.2 (DIC) ±0.0010 & ±0.0024 (pH)	~6 min preparation followed by every ~12 s measurement	~3 week dock deployment

tometry. This method is widely used in laboratory DIC measurements and has been adapted to pCO_2 measurement on buoys and moorings.[22,23] Based on this method, the *in situ* Moored Autonomous DIC (MADIC) system was deployed for surface time-series measurements over 7 months.[15] This method can be complicated for *in situ* deployment at depth due to its use of a gas stream for infrared CO_2 detection.

In the spectrophotometric method, CO_2 from acidified seawater is equilibrated with a pH-sensitive indicator dye across a gas-permeable membrane (e.g., Teflon AF 2400). The absorbance in the CO_2 equilibrated indicator, i.e., indicator pH, is measured spectrophotometrically and can be quantitatively correlated to the sample DIC.[17,18,24−26] The spectrophotometric method is promising for its high sensitivity and ability to provide near-continuous *in situ* DIC measurements.[27] Sensor calibration can be minimized with stable indicator solutions and optical systems. Because this method measures only in the aqueous phase, it is well suited for submerged and pressurized *in situ* applications, including high-frequency time series, spatial mapping, or profiling deployments. This method has been adapted to *in situ* measurements in the Spectrophotometric Elemental Analysis System for DIC (SEAS-DIC)[17] and the original CHANnelized Optical System (CHANOS I), the latter of which can simultaneously measure DIC and pH in a time-series mode with an accuracy and precision of 0.0024 and 0.001 (pH), and 5.2 and 2.5 μmol kg^{-1} (DIC), respectively. However, the measurements are intermittent due to the use of noncontinuous pumps and other engineering design considerations.[18,27]

In this paper, we describe the development of the first *in situ* spectrophotometric DIC sensor, CHANOS II, capable of both continuous (~1 Hz measurement frequency) and intermittent time-series measurements, allowing for deployment from stationary and mobile platforms over various time scales and spatial resolutions. *In situ* time-series deployments in the tidal Pocasset River, MA (August 2021), and surface mapping deployments across Waquoit Bay, MA, reveal tidal, seasonal, and episodic biogeochemical processes. The CHANOS II is the first autonomous, *in situ* sensor with a high enough sampling frequency to allow for real-time profiling and mapping of DIC. *In situ* DIC measurements by CHANOS II are close to climate quality, which allows the sensor to capture many variabilities in dynamic coastal environments.

METHODS

Measurement Principles. The spectrophotometric DIC method for CHANOS II operates by using Teflon AF 2400 capillary tubing as the membrane in a tube-in-tube design, where seawater is acidified and then pumped through the outer shell of the Teflon tubing to equilibrate CO_2 with a countercurrent flowing pH-sensitive indicator of known alkalinity inside the Teflon tubing (see Sensor System below).[18,27] The countercurrent design improves equilibrium efficiency and achieves a fast response time. After equilibration, the DIC of the acidified sample is a function of the CO_2 fugacity (fCO_2) of the equilibrated indicator, such that

$$\log(fCO_2)_{aSW} = \log\left(p \cdot \frac{[DIC]}{(K_0)_{aSW}}\right) = \log(fCO_2)_{ind} \quad (1)$$

where subscript 'aSW' designates the acidified seawater sample, subscript 'ind' designates the indicator, $(K_0)_{aSW}$ is the Henry's Law constant for the acidified sample, and p is the equilibration efficiency (%) for CO_2 equilibration across the semipermeable Teflon AF membrane.[27] p is a function of flow rate, temperature, indicator properties, and fCO_2 gradient and can be experimentally calibrated by determining the percent CO_2 equilibration across the Teflon tubing membrane for a seawater sample of known DIC.[27] In CHANOS II measurements, p of 100% is achieved, indicating full CO_2 equilibration between the acidified sample and the indicator solution across Teflon AF tubing.[18] This serves two purposes: (1) simplifying DIC calibration and calculation by removing the need to calibrate p and (2) slowing the flow rate of indicator solution (allowing more time to equilibrate), which consumes less reagent.

Equilibrated fCO_2 of the indicator solution can be further described by the expression[24,27]

$$\log(fCO_2)_{ind} = B(T) - \log(K_0)_{ind} - \log\left(\frac{R - e_1}{1 - R \cdot (e_3/e_2)}\right) \quad (2)$$

where $B(T)$ describes the chemical and optical properties of the indicator at a given temperature[24,27] (see below). $(K_0)_{ind}$ is the Henry's Law constant for the indicator solution. e_1, e_2, and e_3 are experimentally determined constants representing molar absorbance ratios at wavelengths λ_1 and λ_2, the absorbance maxima for the indicator acid (HI^-) and base (I^{2-}) species. A bromocresol purple (BCP) sulfophthalein pH indicator was used for measurements with λ_1 = 432 and λ_2 = 589 nm. A third nonabsorbing reference wavelength λ_{ref} or λ_3 = 700 nm was used to correct baseline drift during measurements. Constant molar absorbance ratios (e_1 and e_3/e_2) for this indicator have been previously described.[24,27] The absorbance ratio, R, of the indicator solution is defined as

$$R = \frac{A(\lambda_2) - A(\lambda_3)}{A(\lambda_1) - A(\lambda_3)} \quad (3)$$

where $A(\lambda_1)$, $A(\lambda_2)$, and $A(\lambda_3)$ are measured absorbance at the three corresponding wavelengths. In eq 2, $B(T)$ is experimentally determined at a given temperature by measuring the absorbance ratio R of Certified Reference

https://doi.org/10.1021/acsestwater.3c00787
ACS EST Water 2024, 4, 1775−1785

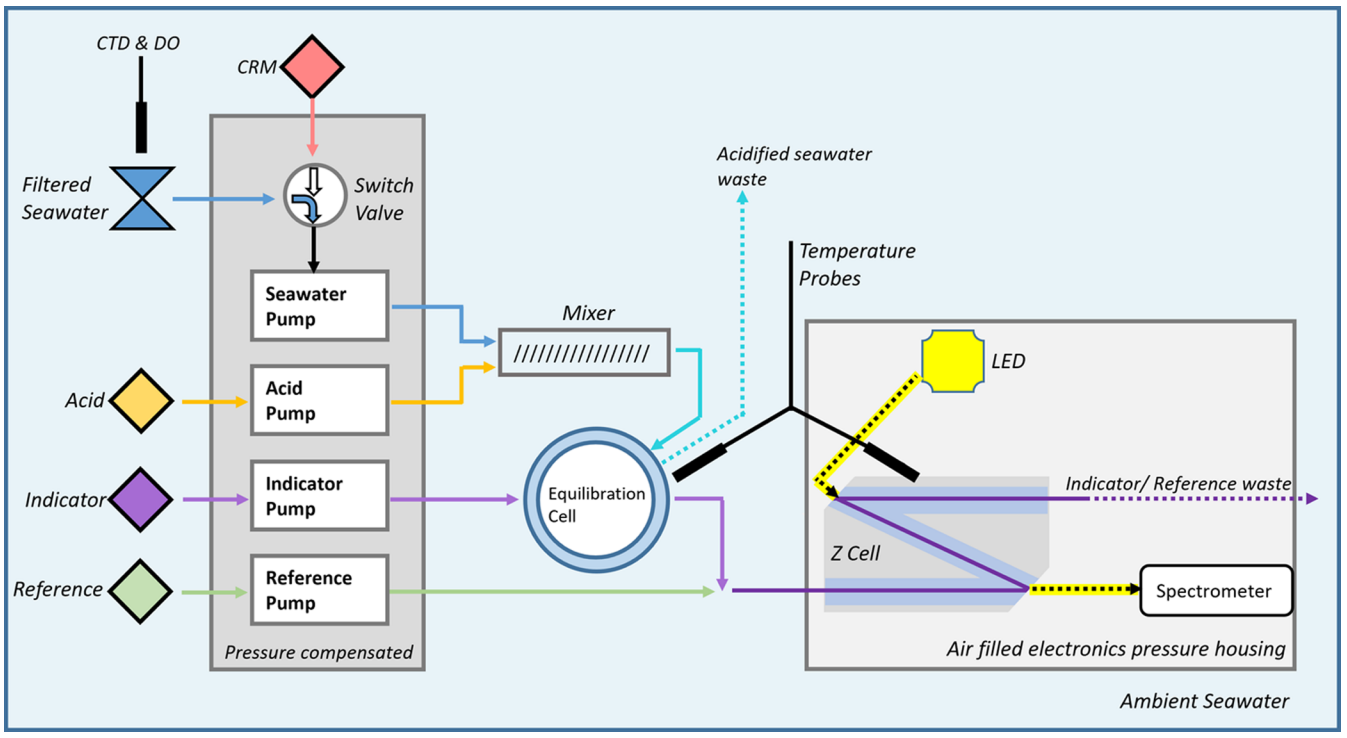

Figure 1. Schematic of the CHANOS II DIC sensor. Reference or indicator solutions are pumped through the optical "Z" cell for optical measurement via a spectrophotometer.

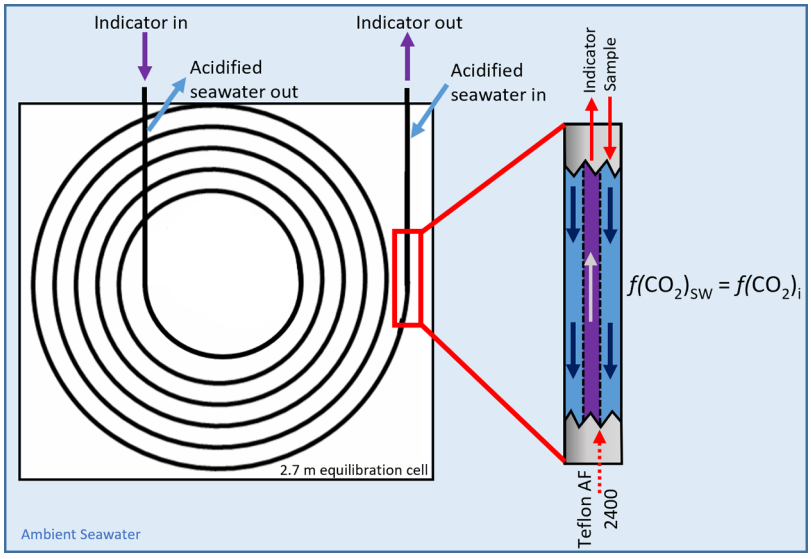

Figure 2. 2-D schematic of the 2.7 m CO_2 equilibration cell (fluidic manifold) used in CHANOS II. The black circles and lines represent the hollow channel holding the Teflon AF 2400 tubing. The red square and lines show the zoomed-in view of Teflon AF tubing inserted in the manifold channel with sample and indicator flow directions.

Materials (CRMs; provided by the Dickson Laboratory at the Scripps Institution of Oceanography) and combining eqs 1 and 2 to solve $B(T)$. $B(T)$ at a given temperature can be described as[24,27]

$$B(T) = \log([\mathrm{TA}] + [H^+] - [I^{2-}]_i) + \log\left(\frac{K_I \cdot e_1}{K_1'}\right)_i \quad (4)$$

where K_I is the indicator dissociation constant, K_1' is the carbonic acid first dissociation constant in the indicator solution, and TA is the total alkalinity of the indicator solution. Since [TA] (~1 mM) is a few orders of magnitude higher than $[H^+]$ and $[I^{2-}]_i$ (a few μM), the first term in eq 4 is essentially determined by indicator solution TA.[24,27,28] If the composition of the indicator solution (i.e., its TA) is stable, then all terms in eq 4, thus $B(T)$, will be constant at a given temperature. The temperature effect on $B(T)$ is directly related to the two dissociation constants in eq 4. In theory, if the indicator solution is stable during the deployment, $B(T)$ does not need to be recalibrated, i.e., calibration-free.

Sensor System. The CHANOS II sensor (Figure 1) uses an array of 4 modified peristaltic pumps (OEM-B02, Baoding

https://doi.org/10.1021/acsestwater.3c00787
ACS EST Water 2024, 4, 1775−1785

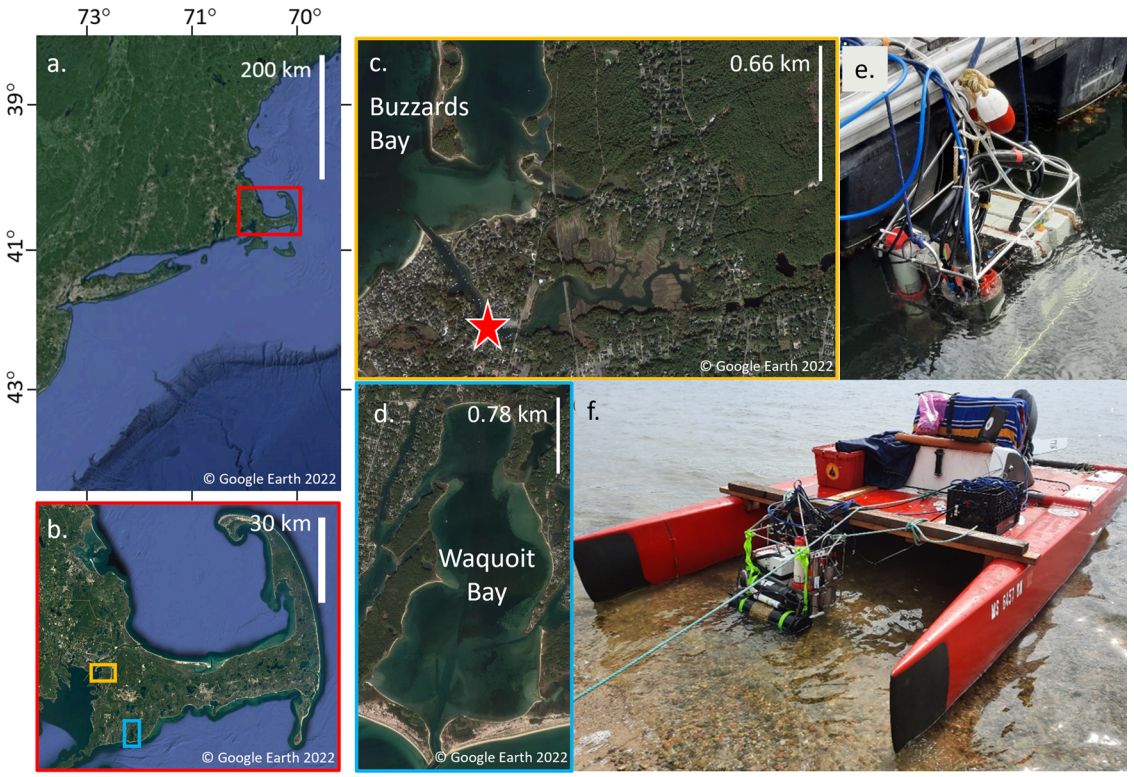

Figure 3. (a) Locations of CHANOS II deployments in the northeastern USA, including (b) Cape Cod, MA, in the enlarged red box. (c) Enlarged yellow-box area in (b) indicates the Pocasset River and surrounding area, MA. (d) Enlarged blue-box area in (b) indicates Waquoit Bay, MA. The red star on panel (c) marks the location of the Scallop Bay Marina deployment of the CHANOS II package, pictured in panel (e). Panel (f) shows the CHANOS II package just after deployment from the TriFly research catamaran at the Waquoit Bay National Estuarine Research Reserve.

Shenchen Precision Pump Co., Ltd., China) with PharMed BPT tubing (1 mm ID, Saint-Gobain, France) and 2 switch valves (T225PK031, NResearch, Inc.) to move seawater, CRMs, hydrochloric acid (HCl), reference, and indicator solutions through the system. These components are packed in custom pressure housings filled with electronic liquid (FC-770, 3M) to compensate for pressure, and the unit was pressure tested to 1200 m. A 2.7 m Teflon AF 2400 semipermeable tubing (0.25 mm ID × 0.51 mm OD, Biogeneral Inc.) is used as the inner shell of a custom-made fluidic manifold functioning as a CO_2 equilibration cell, mimicking the tube-in-tube design used in the original CHANOS, through which reference or indicator solutions are pumped countercurrent to the acidified seawater to achieve efficient flow-through CO_2 equilibration (Figure 2). The manifold simplified the assembly of the equilibration cell and made it more robust. Temperature, salinity, and pressure are monitored by a CTD sensor at the seawater intake (SBE FastCAT 49, Seabird Scientific). Dissolved oxygen (DO) is measured with an Aanderaa 4330 dissolved oxygen optode (Xylem Aanderaa). CHANOS II provides power and records the data for both the CTD and DO sensors.

A separate custom pressure housing contains a 10 mm optical "Z" cell (SMA-Z-10 mm, 26 μL internal volume, FIALab), a mini-spectrophotometer (USB4000, Ocean Optics USA) monitoring in the 300−800 nm wavelength range, controlling electronics, and a white LED light source (LUXEON Rebel LED, MR-WC120-20S, Quadica Developments, Inc., Canada) (Figure 1). The electronic system consists of control boards equipped with an ARM-based microprocessor (TS7600, Technologic Systems). Custom control software runs on the microprocessor and stores data on an internal micro-USB card. The sensor has real-time communication via an Ethernet to a computer. The system runs on 12 V DC power through an external power source or battery (Big-Jim Li-Ion battery, SubCtech, Germany).

A driving principle of this sensor design was to use off-the-shelf components wherever possible to control the cost of the unit itself and to allow for easy replacement of spare parts in the field. The fluidic connections, pressure-compensated pump housings, and optical systems are modular and modifiable, such that this sensor can be adapted for spectrophotometric measurement of other carbonate parameters including pH, pCO_2, and TA.

Reagents. Acid, reference, and indicator solutions, as well as CRM, are carried onboard the sensor at ambient pressure in an off-the-shelf weatherproof plastic box rated by National Electrical Manufacturers Association standards for physical protection and fouling reduction. Seawater is acidified with HCl (3.0 M, diluted from ACS Certified Plus, 36.5 to 38.0%, Fisher Chemical) at an ∼200:1 seawater-to-acid mixing ratio. The reference solution is made from Milli-Q water and extra-pure Na_2CO_3 (ACS Certified, 99.7%+ purity, Fisher Chemical) to achieve a TA content of ∼1000 μmol kg^{-1}. Bromocresol purple sodium salt (90%+ purity, Sigma-Aldrich) is added to the reference solution to make the indicator solution with a concentration of ∼25 μM, optimized for measurement of seawater at DIC concentrations ∼1500 to 3000 μmol kg^{-1} at 1 cm optical path length.[18,24] CRM or secondary standards (local seawater calibrated with CRM), reference, and indicator solutions are stored in gas-impermeable aluminum laminated bags (Calibrated Instruments, Inc.),

https://doi.org/10.1021/acsestwater.3c00787
ACS EST Water 2024, 4, 1775−1785

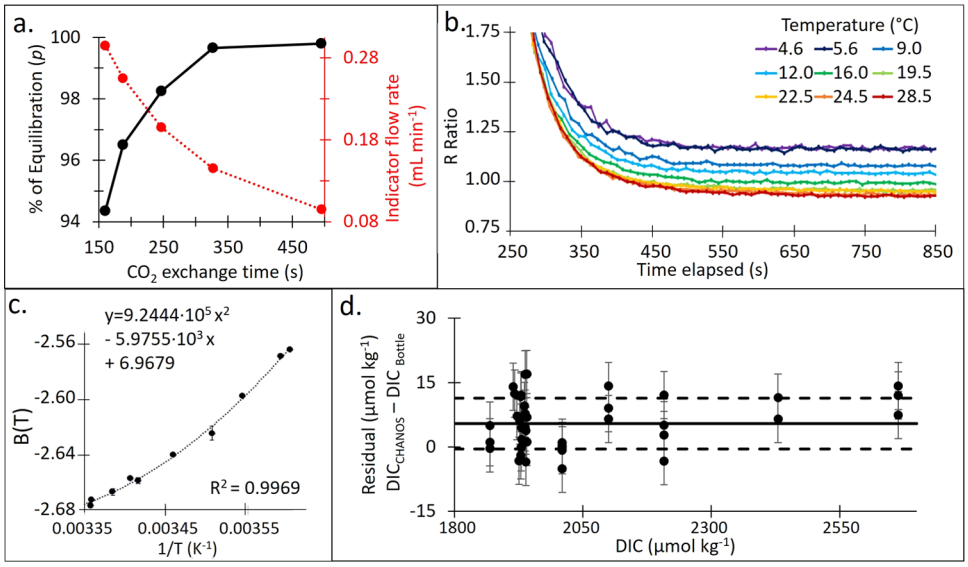

Figure 4. Laboratory test results on CHANOS II's performance and temperature response. Comparison of indicator flow rate and CO_2 equilibration efficiency (p in eq 1) in relationship with CO_2 exchange (equilibration) time (a). Absorbance ratio R vs time for laboratory measurements of a secondary seawater standard at varying temperatures (DIC = 1938 μmol kg^{-1}, salinity = 31) (b). Experimentally derived indicator behavior of $B(T)$ as a function of temperature. (c). Residuals between DIC were measured via bottle samples (DIC_{Bottle}) and CHANOS II (DIC_{CHANOS}) in laboratory tests (d), where three sets of ~20 min continuous measurements were taken by CHANOS II consecutively for each known DIC sample. The horizontal black line in (d) represents the mean at −5.9 μmol kg^{-1}, with a standard deviation of 6.0 μmol kg^{-1} (dashed lines). Error bars represent estimated laboratory precision in CHANOS II measurements (i.e., 5.5 μmol kg^{-1}).

which have been shown to retain the original solution composition for one (CRM) or several (indicator and reference) months at a time.[18]

Calibration. Before each deployment, an experimental $B(T)$ calibration curve was generated to establish the relationship between $B(T)$ and the temperature. This curve is derived from repeated measurements of CRMs or secondary standards in a large water bath under varying temperatures (±0.1 °C). Such a calibration of $B(T)$ may also be conducted *in situ* during a deployment. *In situ* measurements of CRMs or secondary standards by CHANOS II may also serve as quality control of DIC measurements.

Sensor Operation. For a typical sensor operation, the optical cell is first flushed with a reference solution, and a reference spectrum is recorded every few hours to correct for any potential optical drift. An indicator solution is then pumped through the inner Teflon tubing situated in the fluidic channel of the CO_2 equilibration cell (manifold) (Figure 2). Seawater is filtered through nylon and a generic 80-mesh copper screen to reduce fouling and then continuously mixed with acid. The acidified seawater is then pumped into the fluidic manifold channel outside the Teflon tubing, counter-current to the flow of the indicator solution to achieve efficient flow-through CO_2 equilibration. Then, a CO_2-equilibrated indicator is directed into the optical cell where its intensity spectra (300−800 nm) are monitored at ~1 Hz by the spectrophotometer. The sensor records spectra, temperature, and salinity, which are then used to calculate absorbance ratios and seawater DIC (eqs 1 and 2).

CHANOS II measurements can be made in near-continuous or intermittent modes. In near-continuous mode, the sensor can achieve high-frequency (up to ~1 Hz) optical measurements, where indicator solution and acidified seawater are pumped continuously, allowing for time-series or profiling/mapping measurements with occasional interruptions for reference and/or CRM calibrations. In intermittent mode, the sensor will conserve reagents and battery by pumping indicator and acidified seawater for up to 15 min measurements at a time in a user-defined periodic schedule. It is noted that while the sensor records high-frequency spectra measurements at 1 Hz, the response time of the sensor as described in the results section refers to the time required to obtain full CO_2 equilibration between indicator solution and acidified seawater samples across the Teflon tubing. As such, each data point in high-frequency measurements represents a running average of DIC measurements over the last few minutes to approximate the sensor response time.

Ground-Truthing and Field Deployments. *Stationary Time-Series Measurements in the Pocasset River, MA.* CHANOS II was deployed for a total of 59 days with near-continuous or intermittent (hourly) measurements between July 22 and November 14, 2021, from a dock at the Scallop Bay Marina, MA (41.70 N, 70.62 W; Figure 3). This site is ~500 m upstream from the mouth of the small Pocasset River, which flows westward for ~3.2 km through a series of small ponds and salt marshes into Buzzards Bay. The sensor package, including CHANOS II, an Aanderaa 4330 dissolved oxygen (DO) optode, and Ruskin RBR*concerto* CTD, was submerged ~1 m below the surface. Breaks in the time-series of 1 day to 1 week included both routine maintenance (e.g., replacement of batteries, filters, and reagents) and troubleshooting. *In situ* CRM measurements were taken every 6−36 h throughout the deployment.

Bottle DIC samples were collected following the best practices of seawater CO_2 sampling.[29] These samples were used to evaluate CHANOS II's performance. Bottle samples prior to October 28 were filtered with a 0.45 μm capsule filter and poisoned with saturated $HgCl_2$, but those taken after this date were poisoned but not filtered due to power failures at the site. In these cases, samples were analyzed for DIC as rapidly as possible, typically within 1 day of collection. All DIC samples

https://doi.org/10.1021/acsestwater.3c00787
ACS EST Water 2024, 4, 1775−1785

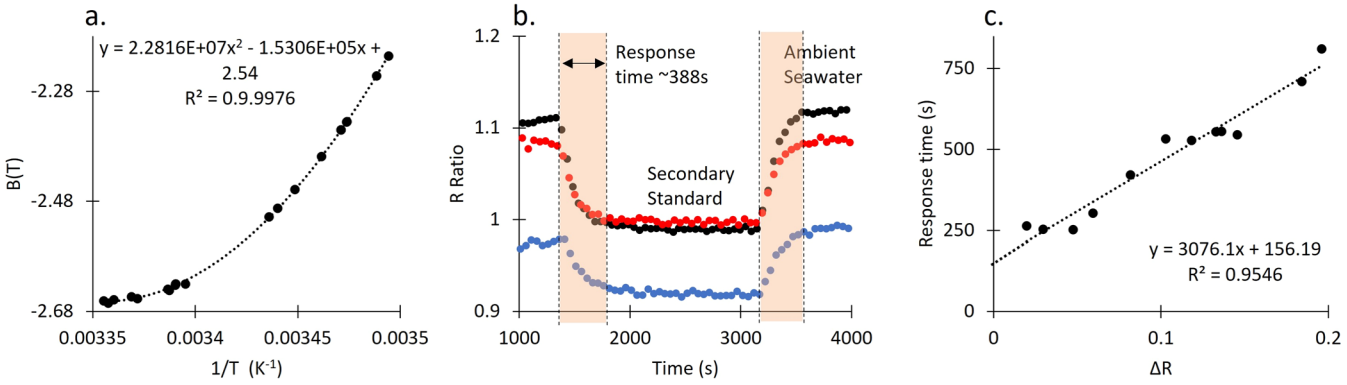

Figure 5. *In situ*-derived indicator behavior of $B(T)$ as a function of temperature during the time-series deployment at the Pocasset River (a). Examples of sensor responses of indicator R ratios (eq 2) to changes between the ambient seawater sample and secondary standards onboard the sensor during deployment (b). The data (three colored data series) were obtained by toggling between ambient seawater and a secondary standard at three-time points when *in situ* calibration occurred. The x-axis denotes a running time in s, where ambient seawater was switched to a secondary standard at the beginning of the first shaded orange bar and back to ambient seawater at the beginning of the second shaded bar. The difference in DIC between the ambient seawater and secondary standard for the blue (bottom) data set was ~150 μmol kg^{-1}. Sensor response time vs the difference in R ratios (ΔR) between toggled ambient DIC samples and onboard secondary seawater standards obtained during the Pocasset River deployment (c). The dashed line represents the best linear fit of the data points.

were measured by a DIC autoanalyzer (AS-C3, Apollo SciTech, DE) with a precision and accuracy of ±0.1%.

Small Boat In Situ Towing, Waquoit Bay, MA. To test the sensor's capability in high-resolution spatial mapping from mobile platforms, the CHANOS II package, including an auxiliary Aanderaa 4330 DO, SBE 37 CTD, and Ruskin RBR*concerto* CTD sensor, was towed just below the surface from the front of the small research catamaran *TriFly* in Waquoit Bay, MA, on September 20, 27, and 28, 2021 (Figure 3). Four towed deployments throughout the bay covered ~13 to 15 km over ~2 h each at an average speed of ~110 m min^{-1}, centered around two high (September 20 and 27) and two low (September 27 and 28) tides. DIC was measured near continuously by CHANOS II, and 80 discrete DIC bottle samples were collected at 5 min intervals for sensor-bottle comparison. These samples were poisoned but not filtered, and they were analyzed in the laboratory within 1 day of collection.

RESULTS AND DISCUSSION

Laboratory Testing and Calibration. CHANOS II was evaluated in the laboratory for repeatability, precision, accuracy, and equilibration efficiency. A comparison of indicator flow rate and CO_2 equilibration efficiency (p in eq 1) is shown in Figure 4a. Herein, we choose a slow indicator flow rate (~0.1 mL min^{-1}), which reduces high backpressure in the Teflon tubing and has the benefits of reducing indicator consumption and achieving $p \sim 100\%$ equilibration. This has the trade-off of a slower response time relative to CHANOS I, which used a higher flow rate (~1 mL min^{-1}) and a thinner-walled Teflon AF tubing (0.4 mm ID × 0.5 mm OD), both of which can increase CO_2 equilibration efficiency.[18] However, the current response time of ~2.6 min, as described in the following sections, is still sufficient for measurements in many dynamic marine environments.

Figure 4b shows the results of repeated laboratory measurements of a secondary standard (DIC ~ 2100 μmol kg^{-1}, calibrated against CRM) at temperatures ranging from 4.6 to 28.5 °C. The experimentally determined polynomial $B(T)$ vs $1/T$ curve fit to the data set in Figure 4b was applied as a temperature calibration curve (Figure 4c) to calculate DIC concentrations during laboratory tests. $B(T)$ increases as the temperature decreases. An accuracy of ~5.9 μmol kg^{-1} was determined from the mean of the differences between sample DIC measured by the CHANOS II and by the DIC autoanalyzer (Figure 4d). The laboratory precision of ±5.5 μmol kg^{-1} was determined by a pooled standard deviation of continuous, repeated measurements of known seawater samples, represented by the error bars in Figure 4d (n = 10 measurements for a given seawater sample of known DIC, with each sample measured by CHANOS II at least 3 times).

***In Situ* Calibration and Response Time.** To accurately determine the temperature effect on the sensor's DIC measurements during deployment, a set of 31 measurements of onboard secondary standards were used to determine an *in situ* $B(T)$ temperature calibration curve ranging from 12 to 22 °C throughout the time-series deployment at the Pocasset River site (Figure 5). A standard error calculated between the best-fit $B(T)$ curve and field-measured data (Figure 5a; 1 SE, $B(T) \pm 0.0012$) corresponds to an uncertainty in DIC of ±5.3 μmol kg^{-1}. The resulting $B(T)$ curve (Figure 5a) was used to calculate DIC concentrations during the CHANOS II field deployment. This curve follows a trend similar to that of the laboratory calibration in Figure 4c but differs in magnitude due to a change in the batch of indicator solution with slightly different TA composition.

The sensor response time during deployments was determined by switching between two distinct DIC samples or between onboard bagged secondary standards and ambient samples (Figure 5b).[18] The response time decreased with the difference in absorbance ratio (ΔR, i.e., ΔDIC; Figure 5b) between two distinct DIC contents (Figure 5c) and ranged between 200 and 800 s. The intercept of the best linear fit in Figure 5c indicates the response time with 100% CO_2 equilibration (~156 s) when DIC changes are continuous (i.e., not abrupt changes by toggling two samples with distinct DIC content), which likely represents the real-world situation. This is significantly longer than the full response time of the original CHANOS sensor (~90 s).[18] The CHANOS II response time is primarily limited by the currently available Teflon AF tubing size (0.25 mm ID × 0.51 mm OD) and wall thickness (0.25 mm) used to construct the CO_2 equilibration cell, versus 0.41 mm ID × 0.56 mm OD in the original

https://doi.org/10.1021/acsestwater.3c00787
ACS EST Water 2024, 4, 1775−1785

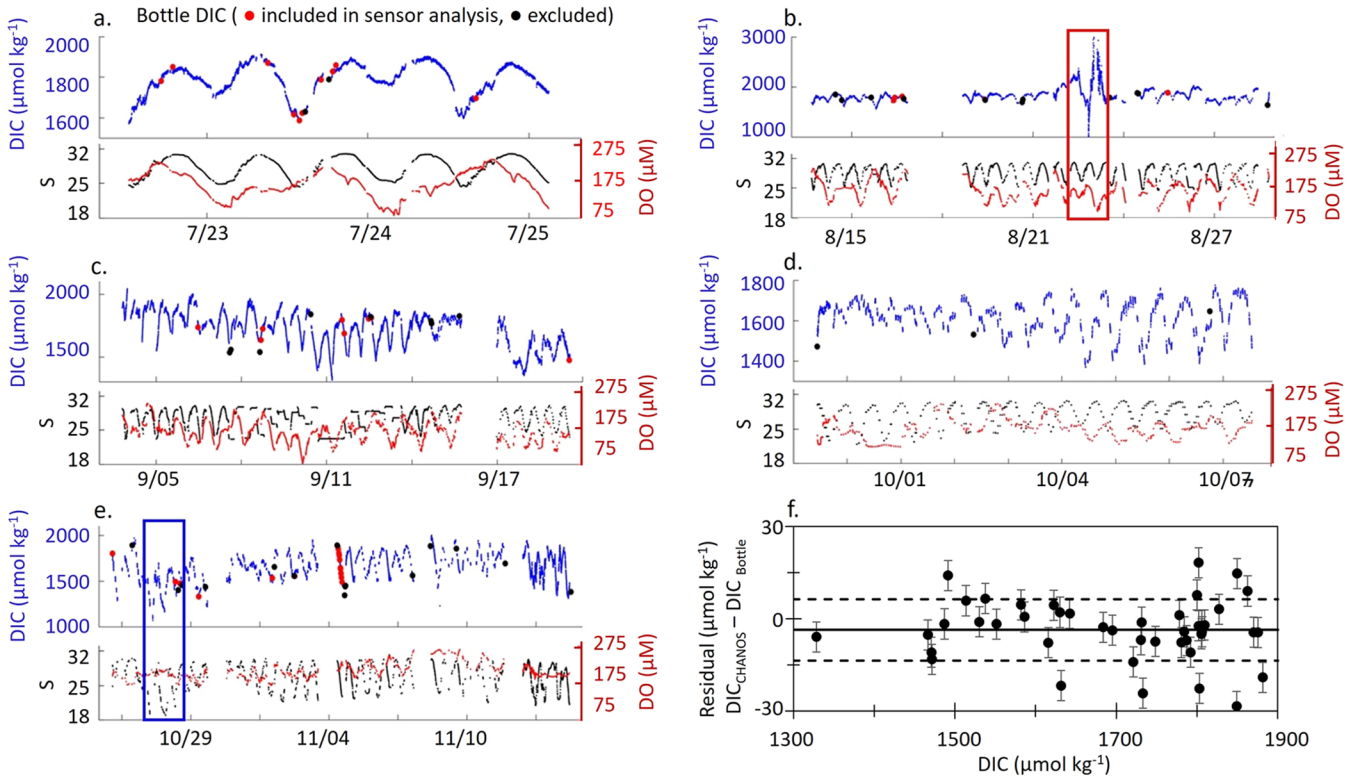

Figure 6. (a–e) CHANOS II time-series data binned by minute (blue), salinity (black), and dissolved oxygen (red) during the Pocasset River deployment (July–November 2021). Bottle sample DIC data are shown as red dots for data used in the sensor evaluation and as black dots for those excluded. The latter wase due to (1) nonsimultaneous sample collection (e.g., if the sensor was taking a reference or standard measurement while a bottle sample was collected) or (2) lack of sample filtration; they were shown for reference. The red box surrounding August 22 corresponds to tropical storm Henri, and the blue box surrounding October 27 indicates a northeastern winter storm. Salinity during the winter storm dropped as low as ∼12, which is cut off in panel (e) for vertical scaling. The full salinity range during this storm is shown in Figure 7. Panel (f) shows residuals between DIC_{Bottle} (red dots in a–e) and DIC_{CHANOS}. The horizontal black line represents the mean at −3.7 μmol kg^{-1}, with a standard deviation (1σ) of 10.0 μmol kg^{-1} (dashed lines). Error bars represent the estimated field *in situ* precision in CHANOS II measurements (i.e., 4.9 μmol kg^{-1}).

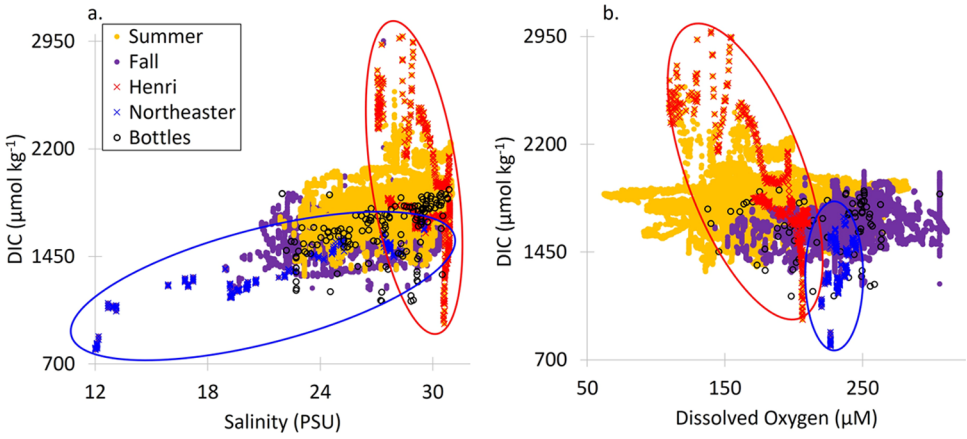

Figure 7. CHANOS II DIC measurements as a function of salinity (a) and dissolved oxygen (b), grouped by color into summer (July–Sept), fall (October–Nov) and storm events during the Pocasset River time-series deployment. Bottle samples are identified by open black circles. The red ovals highlight DIC and DO values measured during tropical storm Henri around August 22, 2021. The blue oval highlights those values during a northeaster storm on October 27, 2021.

CHANOS with a wall thickness of 0.15 mm.[18,27] For stationary time-series deployment where the DIC concentration of ambient seawater changes more gradually, the sensor response is sufficiently fast to capture many variabilities of DIC concentrations in diverse marine environments. The current configuration can also capture many DIC dynamics during a slow-moving mobile deployment. For example, for an ROV moving at 0.2 knots (6.2 m min^{-1}), a running average of DIC measurements over the estimated response time of ∼156 s will capture an attenuated spatial resolution of better than 17 m, which still represents a significant improvement over individual bottle samples. If using the Teflon AF tubing described in the

https://doi.org/10.1021/acsestwater.3c00787
ACS EST Water 2024, 4, 1775–1785

original CHANOS,[18,27] such a spatial resolution will be better than 10 m. Given the limitation in Teflon tubing supply, this should not be a significant constraint of the response time of the sensor over the long term as a more appropriate Teflon tubing can be substituted to achieve better resolution without further modifications.

Pocasset River Time-Series Measurements. The Pocasset River time series resulted in 59 days of CHANOS II DIC data, which were compared to 45 laboratory-analyzed bottle samples collected during the deployment (Figure 6). The DIC recorded during this deployment ranged from ∼1300 to 1900 μmol kg^{-1}, except for the two storm periods described below (Figure 6b and 6e). The residuals between bottle samples and CHANOS II DIC measurements had a mean of −3.7 ± 10.0 (1σ) μmol kg^{-1}, which reflects the combined laboratory analytical error of bottle DIC measurements (±2.0 μmol kg^{-1}) and sensor measurement uncertainty during deployments. If we use the mean residual as the mean uncertainty around true DIC values determined by bottle samples, the sensor has a field accuracy of ±3.7 μmol kg^{-1}, similar to the laboratory-determined accuracy. A pooled standard deviation of 5 min repeated sensor measurements (at ∼1 Hz) indicated a field precision of ±4.9 μmol kg^{-1}, which is consistent with the laboratory-determined precision (±5.5 μmol kg^{-1}).

This time series highlights tidal, seasonal, and episodic biogeochemical changes at this site, including two different DIC responses to a tropical storm and a northeastern winter storm. Tropical storm Henri primarily brought heavy winds and waves to the deployment site on August 22, 2021. The CHANOS record shows that DIC values first decreased as the storm arrived, possibly due to a combination effect of the storm surge of Buzzards Bay water and a certain degree of dilution with the coming rain (highlighted in Figures 6 and 7). This was followed by a DIC increase that may result from disturbance of the sediment and subsurface water as DIC-rich and DO-poor water from these sources were mixed throughout the water column (Figure 7). This was evidenced by extensive wind damage to the vegetation along the riverbanks and turbid water after the storm.

In contrast, the time series also captured a northeastern storm in late October that primarily caused a dilution event. Large volumes of rain and runoff from the surrounding area flushed into the river, resulting in a significantly decreased salinity and DIC during the storm, as highlighted in Figures 6 and 7. At this time in late October, limited biomass remained onshore and no visible damage occurred in the seagrass beds. The generally low DIC and high DO during this storm indicated that sediment likely did not significantly impact the DIC and DO content in the water column, as likely had occurred during tropical storm Henri.

Because bottle sampling was not possible during storm events, sensor evaluation was complicated during these periods. However, baseline absorbance measurements at 700 nm indicated that the optical system operated acceptably, and an autonomous measurement of an onboard secondary CRM during the northeastern storm on October 27 was comparable with the assigned CRM value 1910.1 μmol kg^{-1}, with a difference of only ∼4.3 μmol kg^{-1}. This is consistent with laboratory-determined precision and accuracy. The challenge of traditional bottle sampling during either storm highlights the importance of deploying CHANOS II and other autonomous sensors to capture episodic signals in dynamic environments.

***In Situ* Towing Measurements in Waquoit Bay, MA.** CHANOS II DIC measurements captured high-resolution spatial variability of DIC content in Waquoit Bay during the towing deployment in late September 2021 (Figure 8).

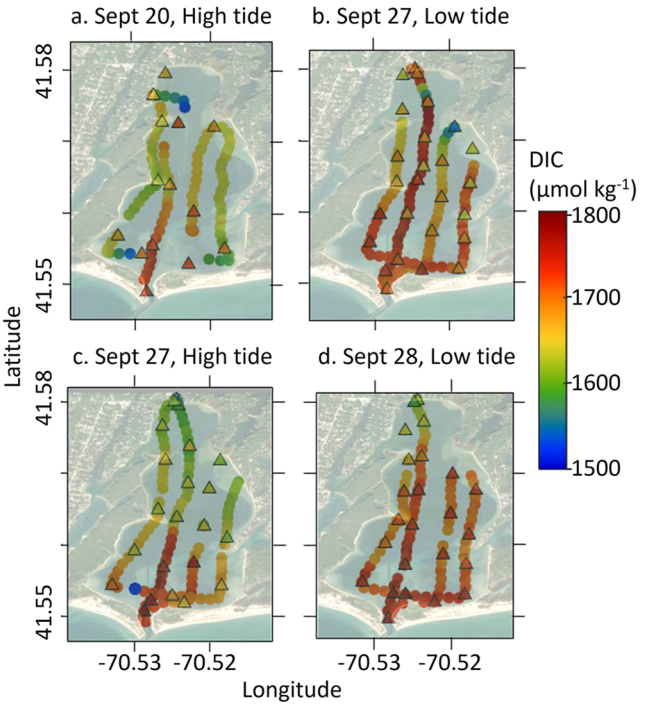

Figure 8. Surface *in situ* DIC measurements by the towed CHANOS II sensor in Waquoit Bay, MA, during high (a, c) and low (b, d) tides in September 2021. The CHANOS II data were binned at 1 min intervals. Bottle samples are denoted in triangles.

CHANOS II data reflect several major local sources of DIC, most notably including the Moonakis and Childs River freshwater endmembers in the north that drain upstream saltwater marshes and ponds and the input of tidal water at the mouth of the bay (Figure 8). DIC ranged between ∼1550 and 1785 μmol kg^{-1} across all deployments, with the highest DIC values observed at the bay mouth and lowest values along the northern edges of the bay. High tide transects (September 20 and 27) had a lower range of DIC values (1550−1765 μmol kg^{-1}) than low tide transects (September 27 and 28) (1600−1785 μmol kg^{-1}), likely reflecting DIC inputs from tidal salt marshes surrounding the bay.[30,31] Multiple endmembers mixing was apparent in the bay, one of which is strongly indicated by low DIC and low salinity water in the northern end of the bay during the high tide on September 27 (Figures 8 and 9). The incoming tidal water from the coast consists of the offshore endmember with relatively high DIC and high DO content compared to the bay water (Figure 9). Elevated DIC paired with lowered DO during low tides and reduced DIC with elevated DO during high tides throughout the bay are consistent with the export of respiratory DIC accompanied by low DO from the surrounding salt marshes through tidal exchange in Waquoit Bay, which may serve as another distinct endmember.[30] Interestingly, an anomalously low DIC (∼1550 μmol kg^{-1}) and high DO (∼130 μM) was recorded in the southwestern portion of the bay during each high tide (but not during low tide) (Figure 8a,c, ∼ 41.555°N, 70.53°W). It is noted that low DIC values (∼1550 μmol kg^{-1}) were also

https://doi.org/10.1021/acsestwater.3c00787
ACS EST Water 2024, 4, 1775−1785

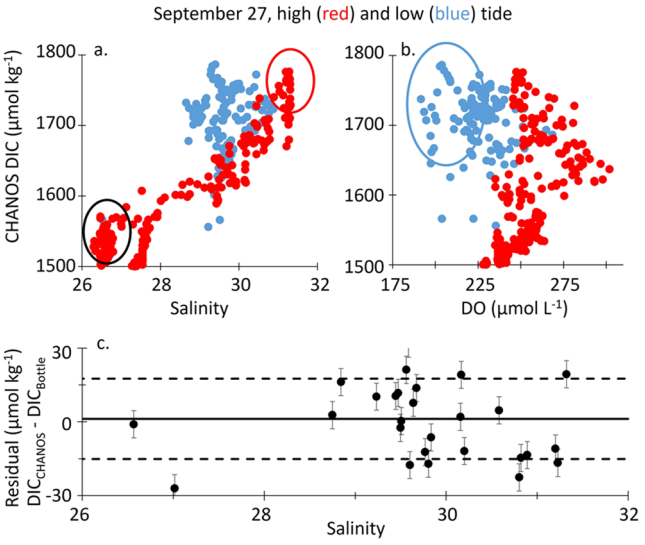

Figure 9. CHANOS II DIC as a function of salinity (a) and DO (b) during the high (red) and low (blue) tide towed deployments across Waquoit Bay on September 27, 2021. The red circle indicates the bay mouth endmember, and the black circle indicates the Moonakis and Childs River endmembers in the northern end of the bay. The blue circle indicates the potential tidal export of DIC from salt marshes with relatively low DO and high DIC. Panel (c) shows the residuals between DIC_{CHANOS} and DIC_{Bottle}, with a mean of 1.2 μmol kg^{-1} (black line) and one standard deviation of 16.3 μmol kg^{-1} (dashed lines). Error bars of data points represent the estimated field-determined precision in CHANOS II measurements (±4.9 μmol kg^{-1}).

reported at high tides during deployment of the RATS DIC system in the northern portion of Waquoit Bay in 2013, potentially indicating groundwater inputs,[19,32] though further investigation is required for our case in the south end of the bay.

The residuals between CHANOS II data and bottle DIC samples collected during the high-resolution surface mapping in Waquoit Bay have a mean of 1.2 μmol kg^{-1} and a standard deviation of 16.3 μmol kg^{-1} (n = 29 bottles) (Figure 9c). This suggests a generally good agreement between the bottle and towed CHANOS II measurements, but with a larger scatter (Figure 9c) than those observed during the Pocasset time series (Figure 6), which may be attributed to several factors. No filtration was used during bottle sample collection during the Waquoit Bay deployment, which may cause higher uncertainty in the bottle DIC analysis. There was an ∼1 m distance between the bottle sampling location and the CHANOS II sample intake. The vibration of the boat may have allowed the movement of air bubbles through the optical cell during DIC measurements, which might cause larger uncertainties in the sensor's measurements. There were 51 bottle samples that were not used for statistical assessment of the sensor performance due to the reasons of poor-quality salinity data from CTD mounting issues (Sept. 20, Sept. 28) or nonsimultaneous collection with CHANOS II data (e.g., during CHANOS II measurement of reference spectra and reference flushing). These bottle data are shown for completeness and indicate general agreement between CHANOS II and bottle measurements (Figure 8). Overall, the high-resolution mapping transects highlight the use of CHANOS II in revealing fine-scale spatial features that may be difficult to capture by traditional bottle samples across tidal cycles.

CONCLUSIONS

This study has detailed the development and field testing of the CHANOS II DIC sensor, a versatile *in situ* sensor capable of both near-continuous and intermittent time-series measurements. Ground-truthing deployments in the Pocasset River and Waquoit Bay have demonstrated these capabilities by CHANOS II. The collected high-resolution data have illuminated biogeochemical signals in dynamic environments that are difficult to capture with traditional bottle measurements. CHANOS II has achieved an accuracy and precision of ±5.9 and ±5.5 μmol kg^{-1}, respectively, in laboratory tests. The mean difference and standard deviation between bottle and sensor measurements were −3.7 ± 10.0 μmol kg^{-1} for time series and 1.2 ± 16.3 μmol kg^{-1} for surface towed deployment at two coastal systems. These are in good agreement with laboratory-determined precision and accuracy. The larger standard deviation around the mean bottle-sensor difference for the towed deployment in Waquoit Bay is mostly due to imperfect sampling procedures and a mismatch of sampling location between the sensor and bottles. The sensor is also capable of calibration *in situ* with CRMs, which is one desirable feature for any *in situ* deployment.

These results reflect a significant improvement from the original CHANOS sensor, retaining a near climate quality measurement quality and allowing for deployments that were not achievable with the previous version, including near-continuous measurements on mobile platforms with lower demand for power, reagents, and maintenance. The CHANOS II is also suited for *in situ* time-series DIC measurements on the order of days to a month without interference. Its broad adaptability for different missions, platforms, and deployment durations is a major advantage of this system for deployment in dynamic environments such as the coastal ocean, where fine-scale spatiotemporal coverage is often desired. Future iterations of this sensor are expected to improve *in situ* precision and accuracy by improving the optical and fluidic systems, as well as the efficiency of CO_2 equilibration.

AUTHOR INFORMATION

Corresponding Author

Zhaohui Aleck Wang − *Department of Marine Chemistry & Geochemistry, Woods Hole Oceanographic Institution, Woods Hole, Massachusetts 02543, United States;* orcid.org/0000-0002-0540-662X; Email: zawang@whoi.edu

Authors

Mallory Ringham − *Department of Marine Chemistry & Geochemistry, Woods Hole Oceanographic Institution, Woods Hole, Massachusetts 02543, United States;* Present Address: Ebb Carbon, Inc., San Carlos, California 94070, United States. mallory@ebbcarbon.com

Frederick Sonnichsen − *Department of Marine Chemistry & Geochemistry, Woods Hole Oceanographic Institution, Woods Hole, Massachusetts 02543, United States*

Steven Lerner − *Department of Marine Chemistry & Geochemistry, Woods Hole Oceanographic Institution, Woods Hole, Massachusetts 02543, United States*

Glenn McDonald − *Department of Marine Chemistry & Geochemistry, Woods Hole Oceanographic Institution, Woods Hole, Massachusetts 02543, United States*

https://doi.org/10.1021/acsestwater.3c00787
ACS EST Water 2024, 4, 1775−1785

Jonathan Pfeifer − *Department of Marine Chemistry & Geochemistry, Woods Hole Oceanographic Institution, Woods Hole, Massachusetts 02543, United States*

Complete contact information is available at: https://pubs.acs.org/10.1021/acsestwater.3c00787

Author Contributions

M.R. and Z.A.W. led the development effort and the writing of the manuscript. All other authors contributed to the sensor development and the edits of the manuscript. All authors have given approval to the final version of the manuscript. CRediT: **Mallory Ringham** conceptualization, data curation, formal analysis, investigation, methodology, validation, visualization, writing-original draft; **Zhaohui Aleck Wang** conceptualization, formal analysis, funding acquisition, investigation, methodology, project administration, supervision, validation, writing-review & editing; **Frederick Sonnichsen** investigation, methodology, resources, validation, writing-review & editing; **Steven Lerner** investigation, resources, software, validation, writing-review & editing; **Glenn McDonald** investigation, methodology, resources, validation, writing-review & editing; **Jonathan Pfeifer** investigation, methodology, resources, validation, writing-review & editing.

Funding

This work was supported by the National Science Foundation (OCE 1233654, OCE-BSF 1635388 and OCE 1841092), the National Oceanic and Atmospheric Administration (NOAA) the Ocean Exploration Research Program (NA18OAR0110352), the NOAA Massachusetts Institute of Technology Sea Grant (2017-R/RCM-51, subaward #5710004253), and Woods Hole Oceanographic Institution Ocean Ventures Funds and Grassle Fellowship Funds.

Notes

The authors declare no competing financial interest.

■ ACKNOWLEDGMENTS

We thank Kate Morkeski, Eyal Wurgaft, and Dylan Titmuss for assistance in CHANOS II deployments; Dan Ward and Matty Paquette for access to the Scallop Bay Marina docks; and Vitalii Sheremet for his work on the *Trifly* deployments.

■ REFERENCES

(1) Cai, W.-J.; Xu, Y.-Y.; Feely, R. A.; et al. Controls on surface water carbonate chemistry along North American ocean margins. *Nat. Commun.* **2020**, *11* (1), No. 2691.

(2) Doney, S. C.; Fabry, V. J.; Feely, R. A.; Kleypas, J. A. Ocean Acidification: The Other CO_2 Problem. *Annu. Rev. Mar. Sci.* **2009**, *1* (1), 169−192.

(3) Millero, F. J. The Marine Inorganic Carbon Cycle. *Chem. Rev.* **2007**, *107*, 308−341.

(4) Wang, Z. A.; Lawson, G. L.; Pilskaln, C. H.; Maas, A. E. Seasonal controls of aragonite saturation states in the Gulf of Maine. *J. Geophys. Res.: Oceans* **2017**, *122*, 372−389.

(5) Bushinsky, S. M.; Takeshita, Y.; Williams, N. L. Observing changes in ocean carbonate chemistry: Our autonomous future. *Curr. Clim. Change Rep.* **2019**, *5*, 207−220.

(6) Martz, T. R.; Daly, K. L.; Byrne, R. H.; Stillman, J. H.; Turk, D. Technology for ocean acidification research: Needs and availability. *Oceanography* **2015**, *25*, 40−47.

(7) Newton, J. A.; Feely, R. A.; Jewett, E. B.; Williamson, P.; Mathis, J. *Global Ocean Acidification Observing Network: Requirements and Governance Plan*, 2nd ed.; GOA-ON, 2015.

(8) Schuster, U.; Hannides, A.; Mintrop, L.; Körtzinger, A. Sensors and instruments for oceanic dissolved carbon measurements. *Ocean Sci.* **2009**, *5*, 547−558.

(9) Orr, J. C.; Epitalon, J. M.; Gattuso, J. P. Comparison of ten packages that compute ocean carbonate chemistry. *Biogeosciences* **2015**, *12*, 1483−1510.

(10) Pierrot, D.; Lewis, E.; Wallace, D. W. R. MS Excel Program Developed for CO2 System Calculations. ORNL/CDIAC-105a; Carbon Dioxide Information Analysis Center, Oak Ridge National Laboratory, U.S. Department of Energy: Oak Ridge, TN, 2006.

(11) Amornthammarong, N.; Ortner, P. B.; Hendee, J.; Woosley, R. A simplified coulometric method for multi-sample measurements of total dissolved inorganic carbon concentration in marine waters. *Analyst* **2014**, *139*, 5263−5270.

(12) Bell, R. J.; Short, R. T.; Byrne, R. H. In-situ determination of total dissolved inorganic carbon by underwater membrane introduction mass spectrometry. *Limnol. Oceanog.: Methods* **2011**, *9*, 164−175.

(13) Chua, E. J.; Savidge, W.; Short, R. T.; Cardenas-Valencia, A. M.; Fulweiler, R. W. A review of the emerging field of underwater mass spectrometry. *Marine Sci.* **2016**, *3*, 209 DOI: 10.3389/fmars.2016.00209.

(14) Colson, B.; Michel, A. C-SPEC: A Deep Sea Laser Spectrometer for Measuring the Carbon System (DIC and pCO_2), *Ocean Sciences Meeting 2022*, Virtual, February 24−March 4, 2022.

(15) Fassbender, A. J.; Sabine, C. L.; Lawrence-Slavas, N.; De Carlo, E. H.; Meinig, C.; Jones, S. M. Robust sensor for extended autonomous measurements of surface ocean dissolved inorganic carbon. *Environ. Sci. Technol.* **2015**, *49*, 3628−3635.

(16) Huang, K.; Cassar, N.; Jönsson, B.; Cai, W. J.; Bender, M. L. An ultrahigh precision, high-frequency dissolved inorganic carbon analyzer based on dual isotope dilution and cavity ring-down spectroscopy. *Environ. Sci. Technol.* **2015**, *49*, 8602−8610.

(17) Liu, X.; Byrne, R. H.; Adornato, L.; Yates, K. K.; Kaltenbacher, E.; Ding, X.; Yang, B. In situ spectrophotometric measurement of dissolved inorganic carbon in seawater. *Environ. Sci. Technol.* **2013**, *47*, 11106−11114.

(18) Wang, Z. A.; Sonnichsen, F. N.; Bradley, A. M.; Hoering, K. A.; Lanagan, T. M.; Chu, S. N.; Hammar, T. R.; Camilli, R. In-situ sensor technology for simultaneous spectrophotometric measurements of seawater total dissolved inorganic carbon and pH. *Environ. Sci. Technol.* **2015**, *49*, 4441−4449.

(19) Sayles, F. L.; Eck, C. An autonomous instrument for time series analysis of TCO_2 from oceanographic moorings. *Deep Sea Res., Part I* **2009**, *56*, 1590−1603.

(20) Nightingale, A. M.; Beaton, A. D.; Mowlem, M. C. Trends in microfluidic systems for in situ chemical analysis of natural waters. *Sens. Actuators, B* **2015**, *221*, 1398−1405.

(21) Tweedie, M.; Sun, D.; Gajula, D. R.; Ward, B.; Maguire, P. D. The analysis of dissolved inorganic carbon in liquid using a microfluidic conductivity sensor with membrane separation of CO_2. *Microfluid. Nanofluid.* **2020**, *24*, 37.

(22) Clarke, J. S.; Achterberg, E. P.; Connelly, D. P.; Schuster, U.; Mowlem, M. Developments in marine pCO_2 measurement technology; towards sustained *in situ* observations. *Trends Anal. Chem.* **2017**, *88*, 53−61.

(23) Sutton, A. J.; Sabine, C. L.; Maenner-Jones, S.; Lawrence-Slavas, N.; Meinig, C.; Feely, R. A.; Mathis, J. T.; Musielewicz, S.; Bott, R.; McLain, P. D. D.; Fought, H. J.; Kozyr, A. A high-frequency atmospheric and seawater pCO2 data set from 14 open-ocean sites using a moored autonomous system. *Earth Syst. Sci. Data* **2014**, *6*, 353−366.

(24) Byrne, R. H.; Liu, X. W.; Kaltenbacher, E. A.; Sell, K. Spectrophotometric measurement of total inorganic carbon in aqueous solutions using a liquid core waveguide. *Anal. Chim. Acta* **2002**, *451*, 221−229.

(25) Clayton, T. D.; Byrne, R. H. Spectrophotometric seawater pH measurement: Total hydrogen ion concentration scale calibration of m-cresol purple and at sea results. *Deep-Sea Res.* **1993**, *40*, 2115−2129.

(26) DeGrandpre, M. D.; Spaulding, R. S.; Newton, J. O.; Jaqueth, E. J.; Hamblock, S. E.; Umansky, A. A.; Harris, K. E. Considerations for the measurement of spectrophotometric pH for ocean acidification and other studies. *Limnol. Oceanogr.: Methods* **2014**, *12*, 830−839.
(27) Wang, Z. A.; Chu, S. N.; Hoering, K. A. High-frequency spectrophotometric measurements of total dissolved inorganic carbon in seawater. *Environ. Sci. Technol.* **2013**, *47*, 7840−7847.
(28) Wang, Z. A.; Liu, X. W.; Byrne, R. H.; Wanninkhof, R.; Bernstein, R. E.; Kaltenbacher, E. A.; Patten, J. Simultaneous spectrophotometric flow-through measurements of pH, carbon dioxide, fugacity, and total inorganic carbon in seawater. *Anal. Chim. Acta* **2007**, *596*, 23−36.
(29) Dickson, A. G.; Sabine, C. L.; Christian, J. R. Guide to Best Practices for Ocean CO2 Measurements. North Pacific Marine Science Organization, 2007 https://epic.awi.de/id/eprint/45690/1/Dickson-etal_2007_Guide_to_Best_Practices_for_Ocean_CO2_Measurement.pdf (accessed Apiril 05, 2021).
(30) Chu, S. N.; Wang, Z. A.; Gonneea, M. E.; Kroeger, K. D.; Ganji, N. K. Deciphering the dynamics of inorganic carbon export from intertidal salt marshes using high-frequency measurements. *Mar. Chem.* **2018**, *206*, 7−18.
(31) Song, S.; Wang, Z. A.; Gonneea, M. E.; Jroeger, K. D.; Chu, S. N.; Li, D.; Liang, H. An important biogeochemical link between organic and inorganic carbon cycling: Effects of organic alkalinity on carbonate chemistry in coastal waters influenced by intertidal salt marshes. *Geochim. Cosmochim. Acta* **2020**, *275*, 123−139.
(32) Martin, W. R.; Sayles, F. L.; McCorkle, D. C.; Weidman, C. Continuous, autonomous measurement of the CO_2 system in Waquoit Bay, MA, In *AGU Fall Meeting Abstracts*, OS53D-07, 2013.

https://doi.org/10.1021/acsestwater.3c00787
ACS EST Water 2024, 4, 1775−1785